

Communication-centric integrated sensing and communications with mixed fields

Yun XIAO*, Enhao WANG, Yunfei CHEN, Hongjian SUN & Aissa IKHLEF

Department of Engineering, Durham University, Durham DH1 3LE, United Kingdom

Received 22 June 2024/Revised 2 September 2024/Accepted 12 September 2024/Published online 15 October 2024

Integrated sensing and communications (ISAC) is expected to play a vital role in the sixth-generation (6G) wireless networks [1]. By utilizing high frequencies, extremely large-scale antenna arrays, and new antenna designs, the 6G-empowered ISAC faces several new challenges, one of which is the considerable near-field (NF) region [1]. Compared with far-field (FF) plane wave model, the NF model assumes spherical wave. This will affect beamforming (BF) designs in ISAC. Most previous works on ISAC beamforming assume the traditional FF model [2]. Recently, the BF design for NF ISAC has also attracted interest [3]. All these studies have considered only the NF or FF model. Ref. [4] considered mixed NF and FF scenario for communications, but without sensing. In practice, the targets and the communication users (CU) could be in different fields. In the mixed near- and far-field, due to their different operating ranges of communications and radar or different mobilities of users and targets, assuming only NF or only FF models causes potential performance loss [5]. Inspired by the observations above, this letter considers a mixed-field ISAC scenario, where the dual-functional base station (BS) serves multiple NF and FF CUs and detects one NF target using mono-static setting. The contributions of the letter include the design of beamformers for the mixed near- and far-field in ISAC and the investigation of the sensing performance loss due to mismatched channel models. The system model is shown in Appendix A. Specifically, a communications performance fairness profile (FPO) problem is formulated, and a Dinkelbach-type successive convex approximation (SCA) algorithm is proposed to solve the problem. Note that using NF models for FF CUs or targets may increase the complexity with little performance improvement. It is beneficial to use FF model for FF target or CU in a mixed-field scenario.

Channel model. Assume that the dual-functional BS employs a uniform linear array (ULA) with N_t transmit antennas and N_r receive antennas. The adjacent antenna spacing is set to $d = \frac{\lambda}{2}$, where λ is the carrier wavelength. Assume that the center of the BS is the origin, and the coordinate of the n -th antenna is $[\delta^{(n)}d, 0]$, where $n = 0, \dots, N_t - 1$, $\delta^{(n)} = n - \frac{N_t-1}{2}$. Assume that the target or CU has distance r and angle $\theta \in [-\frac{\pi}{2}, \frac{\pi}{2}]$ from the origin. The complex channel gain is $\beta = \frac{\beta_0}{r} e^{-j\frac{2\pi}{\lambda}r}$, where β_0 is the 1-meter reference free-space path loss [5]. The Rayleigh distance, denoted as $d_F = \frac{2D^2}{\lambda}$, determines

the boundary between the NF and FF regions, where D is the antenna aperture [3]. When $r < d_F$, the NF channel vector is modeled as $\mathbf{h}_{\text{near}} = \beta \mathbf{a}(r, \theta)$, where $\mathbf{a}(r, \theta)$ is the NF beam focusing vector that can be modeled as $\mathbf{a}(r, \theta) = [e^{-j\frac{2\pi}{\lambda}(r^{(0)}-r)}, \dots, e^{-j\frac{2\pi}{\lambda}(r^{(n)}-r)}, \dots, e^{-j\frac{2\pi}{\lambda}(r^{(N_t-1)}-r)}]^\top$, and $r^{(n)}$ is the distance between the n -th antenna and the target or CU [3]. When $r > d_F$, the FF channel vector is modeled as $\mathbf{h}_{\text{far}} = \beta \mathbf{a}(\theta)$, where $\mathbf{a}(\theta)$ is the FF beam steering vector that can be modeled as $\mathbf{a}(\theta) = [e^{j\frac{2\pi d}{\lambda}\delta^{(0)}\sin(\theta)}, \dots, e^{j\frac{2\pi d}{\lambda}\delta^{(n)}\sin(\theta)}, \dots, e^{j\frac{2\pi d}{\lambda}\delta^{(N_t-1)}\sin(\theta)}]^\top$.

Communications signal-to-interference-plus-noise ratio (SINR). Assume that the system serves multiple single-antenna mixed-field CUs. There are M NF CUs denoted by $m \in \{1, \dots, M\}$, and N FF CUs denoted by $n \in \{1, \dots, N\}$. The CU channels are assumed to be static during L time samples. Note that this letter considers fixed LoS channels with uniform power for all antennas during a given period. This can be extended to NLoS channels, with each antenna having its unique channel gain for future works [6]. The data signal transmitted by the BS is given by

$$\mathbf{x}[l] = \sum_{m=1}^M \mathbf{b}_{\text{near}}^m d_{\text{near}}^m[l] + \sum_{n=1}^N \mathbf{b}_{\text{far}}^n d_{\text{far}}^n[l] = \sum_{j=1}^{M+N} \mathbf{b}_j d_j[l], \quad (1)$$

where $l = 1, \dots, L$, $\{\mathbf{b}_j\} \in \mathcal{C}^{N_t \times 1}$ are the transmit beamforming vectors, $d_j[l] \sim \mathcal{CN}(0, 1)$ are the Gaussian distributed data samples. The received signal at the j -th CU is given by

$$y_j[l] = \underbrace{\mathbf{h}_j^\top \mathbf{b}_j d_j[l]}_{\text{desired signal}} + \underbrace{\mathbf{h}_j^\top \sum_{k \neq j} \mathbf{b}_k d_k[l]}_{\text{interference}} + z_j[l], \quad (2)$$

where $\{\mathbf{h}_j\} = \{\{\mathbf{h}_{\text{near}}^m\} \cup \{\mathbf{h}_{\text{far}}^n\}\}$ are the $N_t \times 1$ channel vectors of CUs, $\{\mathbf{h}_{\text{near}}^m\}$ and $\{\mathbf{h}_{\text{far}}^n\}$ are the channel vectors of NF and FF CUs, respectively, $z_j[l] \sim \mathcal{CN}(0, \sigma_j^2)$ is the additive white Gaussian noise (AWGN) at the j -th CU. The SINR at the j -th CU is given by

$$\Gamma_j = \frac{\mathbf{h}_j^\top \mathbf{b}_j \mathbf{b}_j^\top \mathbf{h}_j^*}{\sum_{k=1, k \neq j}^{M+N} \mathbf{h}_j^\top \mathbf{b}_k \mathbf{b}_k^\top \mathbf{h}_j^* + \sigma_j^2} = \frac{f_j(\{\mathbf{b}_j\})}{g_j(\{\mathbf{b}_j\})}. \quad (3)$$

* Corresponding author (email: yun.xiao@durham.ac.uk)

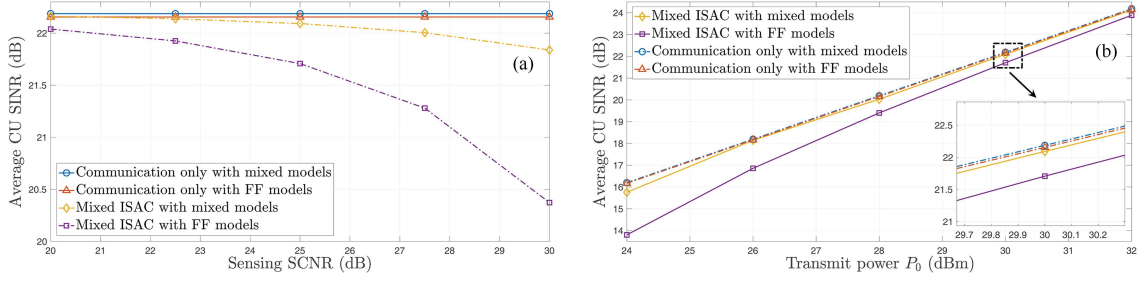


Figure 1 (Color online) (a) Average CU SINR versus SCNR constraint s ; (b) average CU SINR versus P_0 when SCNR constraint = 25 dB.

Sensing signal-to-clutter-plus-noise ratio (SCNR). Using the transmitted signal in (1), the output of the sensing receiver can be expressed as

$$\begin{aligned} y_s[l] &= \mathbf{f}_s^H \beta_s \mathbf{a}_{rs} \mathbf{a}_{ts}^T \mathbf{x}[l] + \mathbf{f}_s^H \sum_{r=1}^R \beta_r \mathbf{a}_{rr} \mathbf{a}_{tr}^T \mathbf{x}[l] + \mathbf{f}_s^H \mathbf{z}_s[l] \\ &= \underbrace{\mathbf{f}_s^H \beta_s \mathbf{A}_s \mathbf{x}[l]}_{\text{sensing signals}} + \underbrace{\mathbf{f}_s^H \sum_{r=1}^R \beta_r \mathbf{A}_r \mathbf{x}[l]}_{\text{clutters}} + \underbrace{\mathbf{f}_s^H \mathbf{z}_s[l]}_{\text{AWGN}}, \end{aligned} \quad (4)$$

where $\mathbf{f}_s \in \mathcal{C}^{N_r \times 1}$ is the receive beamforming vector whose expression can be found in Appendix B. $\mathbf{z}_s[l] \sim \mathcal{CN}(0, \sigma_s^2 \mathbf{I})$ is the AWGN at the sensing receiver, R is the number of clutters. $\mathbf{a}_{ts}, \mathbf{a}_{tr}$ and $\mathbf{a}_{rs}, \mathbf{a}_{rr}$ are the transmit and receive beam focusing vectors, respectively, \mathbf{A}_s and \mathbf{A}_r are the corresponding beam steering or focusing matrices. β_s and β_r are the complex channel gains of the target and clutters, respectively. Then, the SCNR can be expressed as

$$\gamma_s = \frac{\sum_{j=1}^{M+N} |\beta_s|^2 \mathbf{f}_s^H \mathbf{A}_s \mathbf{b}_j \mathbf{b}_j^H \mathbf{A}_s^H \mathbf{f}_s}{\sum_{r=1}^R |\beta_r|^2 \mathbf{f}_s^H \mathbf{A}_r \left(\sum_{j=1}^{M+N} \mathbf{b}_j \mathbf{b}_j^H \right) \mathbf{A}_r^H \mathbf{f}_s + \sigma_s^2 \mathbf{f}_s^H \mathbf{f}_s}. \quad (5)$$

Beamforming design. The optimization problem can be formulated as

$$(P1) \max_{\{\mathbf{b}_j\}} \min_{j=1, \dots, M+N} \frac{\Gamma_j}{c_j} \quad (6a)$$

$$\text{s.t.} \quad \sum_{j=1}^{M+N} \text{tr}(\mathbf{b}_j \mathbf{b}_j^H) \leq P_0, \gamma_s \geq s, \quad (6b)$$

where c_j is the minimum SINR requirement of the j -th CU, s is the minimum SCNR requirement of the target, P_0 is the transmit power constraint. (P1) is non-convex, and to solve it we convert it into a convex one in Appendix C. We propose a Dinkelbach-based SCA algorithm in Appendix D.

Simulation results. We consider that the BS is equipped with $N_t = N_r = 65$ antennas and operates at 28 GHz, resulting in $d_F \approx 21.94$ m. There are two NF CUs, two FF CUs, and one NF target, their locations are listed in Appendix E. The minimum SINR requirement of NF CUs is 15 dB, while for the FF CUs this value is 10 dB. The SCNR constraint is set to 25 dB. P_0 is set to 30 dBm, σ_j^2 and σ_s^2 are set to 1. Both Figures 1(a) and (b) consider four cases, including the communications only systems with mixed or FF channel models and mixed ISAC systems with mixed or FF channel models. Figure 1(a) shows the effect of sensing SCNR on the average CU SINR. One sees that for both mixed ISAC systems, the average SINR decreases with the sensing SCNR.

The average SINR of communication only systems remains flat as the sensing SCNR constraint increases, because they are not affected by the sensing target. The systems with mixed models have higher average CU SINR than those with traditional FF models. The difference between mixed ISAC systems with mixed models and FF models increases dramatically as the sensing SCNR constraint increases. This is expected, as for NF CUs and the NF target, the transmit energy focuses on the locations of CUs and the target, respectively, resulting in reduced energy leakage to the interferers and clutters.

Figure 1(b) shows the effect of total transmit power on the average CU SINR. In all four cases, the average SINR increases with the total transmit power P_0 . The systems with mixed models have higher average SINR than those with FF models. The communication only systems have higher average SINR than mixed ISAC systems. As the total transmit power increases, the gap between systems using mixed models and FF models decreases. This is because higher transmit power enhances overall communication quality, which is particularly beneficial in cases with mismatched models.

Acknowledgements This work is supported in part by EP-SRC TITAN (Grant Nos. EP/Y037243/1, EP/X04047X/1).

Supporting information Appendixes A–E. The supporting information is available online at info.scichina.com and link.springer.com. The supporting materials are published as submitted, without typesetting or editing. The responsibility for scientific accuracy and content remains entirely with the authors.

References

- Liu F, Cui Y H, Masouros C, et al. Integrated sensing and communications: toward dual-functional wireless networks for 6g and beyond. *IEEE J Select Areas Commun*, 2022, 40: 1728–1767
- Chen L, Wang Z, Du Y, et al. Generalized transceiver beamforming for DFRC with MIMO radar and MU-MIMO communication. *IEEE J Select Areas Commun*, 2022, 40: 1795–1808
- Wang Z L, Mu X D, Liu Y W. Near-field integrated sensing and communications. *IEEE Commun Letter*, 2023, 27: 2048–2052
- Zhang Y P, You C S, Chen L, et al. Mixed near- and far-field communications for extremely large-scale array: an interference perspective. *IEEE Commun Letter*, 2023, 27: 2496–2500
- He J, Li L N, Shu T, et al. Mixed near-field and far-field source localization based on exact spatial propagation geometry. *IEEE Trans Veh Technol*, 2021, 70: 3540–3551
- Zhi K D, Pan C H, Ren H, et al. Performance analysis and low-complexity design for XL-MIMO with near-field spatial non-stationarities. *IEEE J Select Areas Commun*, 2024, 42: 1656–1672